Editors: Isabel Beichl, isabel.beichl@nist.gov
Julian V. Noble, jvn@virginia.edu

FITTING NATURE'S BASIC FUNCTIONS PART III: EXPONENTIALS, SINUSOIDS, AND NONLINEAR LEAST SQUARES

By Bert W. Rust

IN PART I[1] AND PART II[2] OF THIS SERIES, WE USED LINEAR LEAST SQUARES TO FIT POLYNOMIALS OF VARIOUS DEGREE TO THE ANNUAL GLOBAL TEMPERATURE ANOMALIES FOR 1856 TO 1999. Polynomials are much beloved by mathematicians but are of limited value for modeling measured data. Natural processes often display linear trends, and occasionally a constant acceleration process exhibits quadratic variation. However, higher-order polynomial behavior is rare in nature, which is more likely to produce exponentials, sinusoids, logistics, Gaussians, or other special functions. Modeling such behaviors with high-order polynomials usually gives spurious wiggles between the data points, and low-order polynomial fits give nonrandom residuals. We saw an example of this syndrome in Figure 4 of Part I, where we attempted to model a quasicyclic variation with a fifth-degree polynomial. That example also illustrated that polynomial fits usually give unrealistic extrapolations of the data.

Fitting an exponential

Consider the problem of fitting an exponential function

$$y(t) = C_0 e^{\beta t}, \tag{1}$$

with unknown parameters C_0 and β, to a set of measured points $\{(t_i, y_i), i = 1, 2, \ldots, m\}$ with additive random errors ϵ_i in the y_i. Because $y(t)$ depends nonlinearly on β, making the fit by linear least squares is impossible. Linearization is possible by taking natural logarithms,

$$\ln[y(t)] = \ln(C_0) + \beta t \equiv L_0 + \beta t, \tag{2}$$

but a linear fit of this model does not give the same result as a nonlinear fit of the original.

As an example, we consider the record of fossil-fuel CO_2 emissions compiled by Gregg Marland, Thomas Boden, and Robert Andres.[3] You can obtain these data at http://cdiac.ornl.gov/trends/emis/em_cont.htm. Figure 1 plots the annual total global emissions, expressed in megatons of carbon, as discrete points. Figure 2 plots the natural logarithms of these totals; the dashed line represents a linear least squares fit of

$$\ln[y(t - t_0)] = L_0 + \beta(t - t_0), \tag{3}$$

with $t_0 = 1856.0$ chosen for consistency with our previous global temperature fits. The parameter estimates were

$$\begin{aligned} \hat{L}_0 &= (4.261 \pm .018)\left[\ln(\text{Mt C})\right], \\ \hat{\beta} &= (3.536 \pm .024) \times 10^{-2}\left[\text{yr}^{-1}\right]. \end{aligned} \tag{4}$$

The fit confirms the growth's basically exponential character, despite the systematic variations around the straight line. We will address those variations later. For now, we note that the back transformed function

$$\hat{y}(t - t_0) = e^{\hat{L}_0} e^{\hat{\beta}(t - t_0)}, \tag{5}$$

plotted as a dashed curve in Figure 1, does not track the data nearly so well as the solid curve, which we obtained by a nonlinear fit of

$$y(t - t_0) = C_0 e^{\beta(t - t_0)}, \tag{6}$$

which gave the parameter estimates

$$\begin{aligned} \hat{C}_0 &= (151.5 \pm 7.5)\left[\text{Mt C}\right], \\ \hat{\beta} &= (2.750 \pm .039) \times 10^{-2}\left[\text{yr}^{-1}\right]. \end{aligned} \tag{7}$$

Although the mathematical models in Equations 3 and 6 are equivalent, the statistical models

$$y_i = C_0 e^{\beta(t_i - t_0)} + \epsilon_i, i = 1, 2, \ldots m \tag{8}$$

$$\ln[y_i] = \ln\left[C_0 e^{\beta(t_i - t_0)}\right] + \dagger_i, i = 1, 2, \ldots m \tag{9}$$

are not.

 1521-9615/02/$17.00 © 2002 IEEE

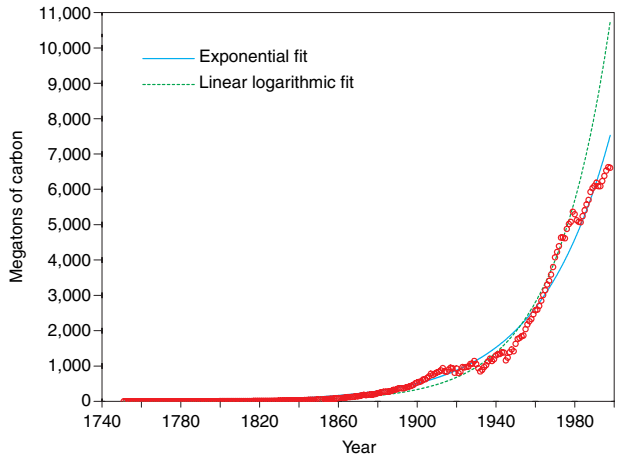

Figure 1. Nonlinear exponential and back-transformed linear logarithmic fits to annual global fossil fuel emissions, 1751–1998.

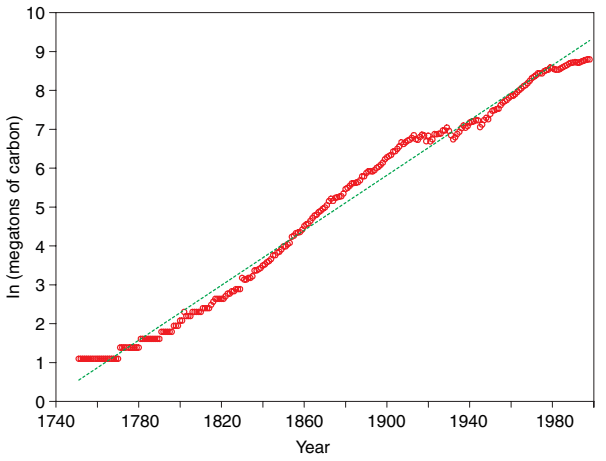

Figure 2. A straight-line fit to the natural logarithms of the annual global total fossil fuel emissions.

Nonlinear least squares

When the mathematical model

$$y(t) = \phi(t, \alpha) \equiv \phi(t, \alpha_1, \alpha_2, \ldots, \alpha_n) \tag{10}$$

depends nonlinearly on one or more of the α_j, the minimization problem

$$R^2(\alpha^*) = \min_{\alpha}\left\{R^2(\alpha)\right\} \equiv \min_{\alpha}\left\{\sum_{i=1}^{m}\left[y_i - \phi(t_i,\alpha)\right]^2\right\} \tag{11}$$

does not admit a closed form estimate for α^*. In fact, $R^2(\alpha)$ will often have more than one *local minimum*, only one of which gives a good fit. Algorithms to estimate α^* are iterative, beginning with initial estimates α_0 and proceeding by a series of corrections,

$$\alpha_{v+1} = \alpha_v + \delta\alpha_v, \tag{12}$$

that obtain each $\delta\alpha_v$ by solving a linear minimization problem. The estimates in Equation 4 gave the initial values used for the nonlinear fit in Figure 1. Convergence to the estimates in Equation 7 required 45 iterations.

To explain the iteration, we assume that v steps have carried the approximation to $\hat{\alpha}_v$. Ideally, the next $\delta\hat{\alpha}_v$ would be chosen to minimize

$$\mathcal{L}_v(\delta\alpha) = \sum_{i=1}^{m}\left[y_i - \phi(t_i, \hat{\alpha}_v + \delta\alpha)\right]^2, \tag{13}$$

but this is just another way of writing the intractable problem in Equation 11. We define m-vectors $\mathbf{y}$ and $\phi(\alpha)$ by

$$\mathbf{y} \equiv (y_1, y_2, \ldots, y_m)^T \tag{14}$$

$$\phi(\alpha) \equiv (\phi(t_1, \alpha), \phi(t_2, \alpha), \ldots, \phi(t_m, \alpha))^T, \tag{15}$$

so that we can write Equation 13 as

$$\mathcal{L}_v(\delta\alpha) = \left[\mathbf{y} - \phi(\hat{\alpha}_v + \delta\alpha)\right]^T\left[\mathbf{y} - \phi(\hat{\alpha}_v + \delta\alpha)\right]. \tag{16}$$

To get something that we can minimize, we will replace $\phi(\hat{\alpha}_v + \delta\alpha)$ with the multivariate, first-order Taylor series approximation

$$\phi(\hat{\alpha}_v + \delta\alpha) \approx \phi(\hat{\alpha}_v) + \mathbf{J}(\hat{\alpha}_v)\delta\alpha, \tag{17}$$

where $\mathbf{J}(\hat{\alpha}_v)$ is the $m \times n$ *Jacobian matrix* with elements

$$J_{i,j}(\hat{\alpha}_v) = \left.\frac{\partial\phi(t,\alpha)}{\partial\alpha_j}\right|_{(t,\alpha)=(t_i,\hat{\alpha}_v)}, \quad i = 1, 2, \ldots, m, \quad j = 1, 2, \ldots, n, \tag{18}$$

To compress the notation further, let $\hat{\phi}_v \equiv \phi(\hat{\alpha}_v)$ and $\hat{\mathbf{J}}_v \equiv \mathbf{J}(\hat{\alpha}_v)$, so the Taylor series approximation becomes

$$\phi(\hat{\alpha}_v + \delta\alpha) \approx \hat{\phi}_v + \hat{\mathbf{J}}_v\delta\alpha. \tag{19}$$

Substituting this expression into Equation 16 gives

$$\mathcal{L}_v(\delta\alpha) = \left[\left(\mathbf{y} - \hat{\phi}_v\right) - \hat{\mathbf{J}}_v\delta\alpha\right]^T\left[\left(\mathbf{y} - \hat{\phi}_v\right) - \hat{\mathbf{J}}_v\delta\alpha\right] \tag{20}$$

for the function to be minimized. It has the same form as the linear least-squares objective function (Part I, Equation 22), so we can estimate the minimum in the same way:

$$\frac{\partial\left[\mathcal{L}_v(\delta\alpha)\right]}{\partial(\delta\alpha)} = \mathbf{0} \;\Rightarrow\; \delta\hat{\alpha}_v = \left[\hat{\mathbf{J}}_v^T\hat{\mathbf{J}}_v\right]^{-1}\hat{\mathbf{J}}_v^T\left(\mathbf{y} - \hat{\phi}_v\right), \tag{21}$$

which is analogous to Equation 26 in Part I. The corrected estimate, $\hat{\alpha}_{v+1} = \hat{\alpha}_v + \delta\hat{\alpha}_v$, will hopefully be closer to α^* than was $\hat{\alpha}_v$. Such an improvement is not guaranteed, so the step is usually shortened to

$$\hat{\alpha}_{v+1} = \hat{\alpha}_v + \lambda\delta\hat{\alpha}_v,\; 0 < \lambda \le 1, \tag{22}$$

where the *step factor* λ is adjusted to guarantee that $R^2(\hat{\alpha}_{v+1}) < R^2(\hat{\alpha}_v)$. The iteration might still converge to a local minimum that does not give a good fit. The only recourse then is to start again with a new α_0.

The above procedure is called the *Gauss-Newton iteration*. In practice it is usually modified to accelerate convergence. The commonly used Levenberg-Marquardt variant effectively replaces Equation 21 with

$$\delta\hat{\alpha}_v = \left[\hat{\mathbf{J}}_v^T\hat{\mathbf{J}}_v + \tau^2\mathbf{D}\right]^{-1}\hat{\mathbf{J}}_v^T\left(\mathbf{y} - \hat{\phi}_v\right), \tag{23}$$

where $\mathbf{D}$ is a suitably chosen diagonal matrix and τ^2 is an adjustable *damping constant*. The calculation actually works with a QR factorization

$$\begin{pmatrix}\hat{\mathbf{J}}\\ \tau\mathbf{D}\end{pmatrix} = \mathbf{Q}\begin{pmatrix}\mathbf{R}\\ \mathbf{O}\end{pmatrix}, \tag{24}$$

analogous to Equation 27 in Part I.

At each step we need to compute both the m values $\phi(t_i, \hat{\alpha}_v)$ and the $m \times n$ partial derivatives $\partial\phi(t_i, \hat{\alpha}_v) / \partial\alpha_j$. For the nonlinear fit in Figure 1, if

$$\phi(t, \alpha) \equiv \alpha_1 e^{\alpha_2(t - t_0)},\; \hat{\alpha}_v \equiv \left(\alpha_1^{(v)}, \alpha_2^{(v)}\right)^T, \tag{25}$$

the required partial derivatives values are

$$\frac{\partial\phi(t_i, \hat{\alpha}_v)}{\partial\alpha_1} = e^{\alpha_2^{(v)}(t_i - t_0)}, \tag{26}$$

$$\frac{\partial\phi(t_i, \hat{\alpha}_v)}{\partial\alpha_2} = \alpha_1^{(v)}(t_i - t_0)e^{\alpha_2^{(v)}(t_i - t_0)}. \tag{27}$$

We can use numerical derivatives $\Delta\phi / \Delta\alpha_j$ if we properly choose $\Delta\alpha_j$, and the iteration will usually converge despite the loss of accuracy at each step.

Estimating uncertainties

The linear least-squares objective function (Part I, Equation 22),

$$\mathcal{L}_{LLS}(\alpha) = (\mathrm{y} - \Phi\alpha)^T(\mathrm{y} - \Phi\alpha), \tag{28}$$

defines a quadratic response surface with a unique minimum *sum of squared residuals* (SSR—Part I, Equations 3 and 5) at

$$\hat{\alpha} = \left(\Phi^T\Phi\right)^{-1}\Phi^T\mathbf{y}, \tag{29}$$

so we can also write it as

$$\mathcal{L}_{LLS}(\alpha) = \mathrm{SSR} + \left(\alpha - \hat{\alpha}\right)^T\Phi^T\Phi\left(\alpha - \hat{\alpha}\right). \tag{30}$$

The function $R^2(\alpha)$ is more complicated than a quadratic bowl, but we can regard each of the $L_v(\delta\alpha)$ as a local quadratic approximation to $R^2(\alpha)$, which we have reparameterized by shifting the origin to $\hat{\alpha}_v$. Let $\hat{\alpha}$ be the final converged estimate of α^*. We can write the local quadratic approximation at the minimum as

$$R^2(\alpha) \approx R^2(\hat{\alpha}) + \left(\alpha - \hat{\alpha}\right)^T\mathbf{J}^T(\hat{\alpha})\mathbf{J}(\hat{\alpha})(\alpha - \hat{\alpha}), \tag{31}$$

which is analogous to Equation 30. Accordingly, we can construct approximations of the statistical diagnostics and tests discussed in Part II by taking $\mathrm{SSR} = R^2(\hat{\alpha})$ and using $\left[\mathbf{J}^T(\hat{\alpha})\mathbf{J}(\hat{\alpha})\right]^{-1}$ for $(\Phi^T\Phi)^{-1}$. This is how we approximated the $\pm1\sigma$ uncertainties in Equation 7. Such approximations are reliable only if Equation 31 is a good approximation to $R^2(\alpha)$ in the neighborhood of α^*. So, it is advisable to use analytic derivatives rather than $\Delta\phi / \Delta\alpha_j$ approximations in calculating $\left[\mathbf{J}^T(\hat{\alpha})\mathbf{J}(\hat{\alpha})\right]^{-1}$. Also, $\pm1\sigma$ confidence intervals will probably be more reliable than $\pm3\sigma$ intervals.

This and the preceding sections have given only the briefest introduction to nonlinear regression. Readers who want more details might like the excellent text by Douglas Bates and Donald Watts.[4]

Global temperatures again

Figure 3 gives an updated record of 146 annual global temperatures for 1856 to 2001. It is obtainable from www.cru.uea.ac.uk/cru/cru.htm, which is maintained by Phil Jones at the University of East Anglia. The dotted and dashed curves are updates to linear least-squares fits done in Parts I and II. They correspond to the first two models in the array

$$y(t) = \phi(t,\alpha) = \alpha_1 + \alpha_2 \begin{Bmatrix} t - t_0 \\ (t - t_0)^2 \\ \exp\left[\hat{\beta}(t - t_0)\right] \\ \exp\left[\alpha_3(t - t_0)\right] \end{Bmatrix}, \quad (32)$$

where $t_0 = 1856.0$. The solid curve corresponds to the third model, which contains an exponential with fixed-rate constant $\hat{\beta} = 2.750 \times 10^{-2}\,\mathrm{yr}^{-1}$—the value Equation 7 estimated for the rate of growth in fossil-fuel emissions. We consider this model because the buildup of fossil-fuel CO_2 in the atmosphere is a possible cause of the global warming. Because $\hat{\beta}$ is fixed, the third fit is also done by linear least squares. In the fourth model, the rate constant is an adjustable parameter, so nonlinear least squares is required. The fitted curve falls roughly halfway between the reduced quadratic and fixed-rate exponential but is not plotted, to reduce the clutter. The fits are extrapolated through the year 2026.

Table 1 gives the parameter estimates and some statistical diagnostics for the fits. The only estimate with doubtful statistical significance is $\hat{\alpha}_2 = (3.7 \pm 1.8) \times 10^{-2}$, for the adjustable-rate exponential. The correlation matrix,

$$\hat{\mathbf{C}} = \begin{pmatrix} 1.000 & -0.934 & 0.904 \\ -0.934 & 1.000 & -0.994 \\ 0.904 & -0.994 & 1.000 \end{pmatrix}, \quad (33)$$

exhibits a high $\hat{\alpha}_2$, $\hat{\alpha}_3$ cross-correlation, which indicates that the data cannot support all the parameters. Let's apply the F-test to compare the SSR for models 3 and 4. Equation 29 in Part II,

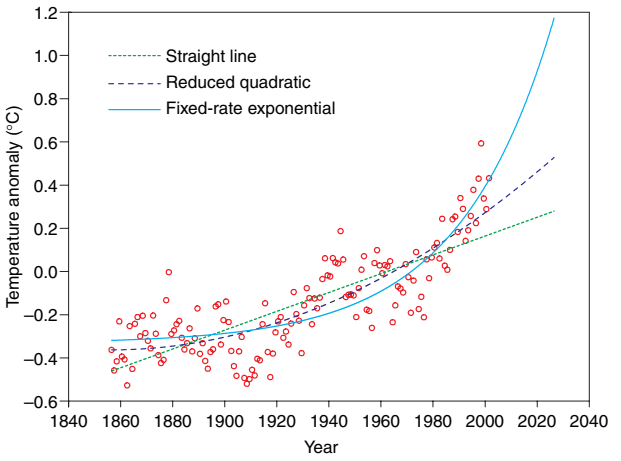

Figure 3. Two-parameter linear least-squares fits to the annual global average temperature anomalies, 1856–2001.

$$u = \frac{(\mathrm{SSR})_H - (\mathrm{SSR})_F}{(\mathrm{SSR})_F} \cdot \frac{m - n}{k}, \quad (34)$$

gives

$$u = \frac{2.195375 - 2.143582}{2.143582} \cdot \frac{146 - 3}{1} = 3.455. \quad (35)$$

So, $u < F_{0.95}(1, 143) = 3.907$, which indicates that $\exp\left[\hat{\alpha}_3(t - t_0)\right]$ is not significantly better than $\exp\left[\hat{\beta}(t - t_0)\right]$. The same comparison between models 2 and 4 gives $u = 5.4876 > F_{0.95}(1, 143)$, which indicates a significant reduction in SSR, but this is not strong evidence for exponential warming.

Fitting sinusoids

The Fourier spectra of the residuals for the fits in Table 1 were dominated by a cycle with a period of approximately 63 years (see Figures 2 and 4 in Part II). In fitting a model of the form

Table 1. Parameter estimates and statistics for baseline fits to annual temperature data.

	Model 1 Straight line	Model 2 Reduced quadratic	Model 3 Fixed-rate exponential	Model 4 Adjustable-rate exponential
$\hat{\alpha}_1$ [°C]	–0.463 ± .023	–0.363 ± .015	–0.333 ± .014	–0.385 ± .037
$\hat{\alpha}_2$ [°C/–]	$(4.36 \pm .28) \times 10^{-3}$	$(3.06 \pm .16) \times 10^{-5}$	$(1.385 \pm .072) \times 10^{-2}$	$(3.7 \pm 1.8) \times 10^{-2}$
$\hat{\alpha}_3$ [yr^{-1}]				$(2.07 \pm .33) \times 10^{-2}$
SSR	2.841397	2.225842	2.195375	2.143582
$100R^2$	63.40%	71.33%	71.72%	72.39%
Cycle [yr]	62.5	61.5	64.5	63.5

Table 2. Parameter estimates and statistics for (baseline + sinusoid) fits to annual global temperature data.

	Model 1 Straight line	Model 2 Reduced quadratic	Model 3 Fixed-rate exponential	Model 4 Adjustable-rate exponential
$\hat{\alpha}_1$ [°C]	–0.488 ± .021	–0.375 ± .014	–0.349 ± .014	–0.469 ± .053
$\hat{\alpha}_2$ [°C/–]	$(4.59 \pm .26) \times 10^{-3}$	$(3.18 \pm .16) \times 10^{-5}$	$(1.502 \pm .077) \times 10^{-2}$	$(8.0 \pm 3.5) \times 10^{-2}$
$\hat{\alpha}_3$ [yr^{-1}]				$(1.60 \pm .28) \times 10^{-2}$
$\hat{T}$ [yr]	63.0 ± 1.9	63.1 ± 1.9	67.4 ± 2.4	64.9 ± 2.1
$\hat{A}$ [°C]	0.117 ± .014	0.105 ± .012	0.094 ± .014	0.102 ± .013
$\hat{\theta}$ [yr]	–4.2 ± 2.4	–6.6 ± 2.3	–4.6 ± 2.9	–5.1 ± 2.4
SSR	1.881892	1.478319	1.630168	1.476133
$100R^2$	75.76%	80.96%	79.00%	80.98%
u	23.964	23.766	16.296	21.101

$$\phi(t,T,A,\theta) = A\sin\left[\frac{2\pi}{T}(t+\theta)\right], \tag{36}$$

it is usually more convenient to define new parameters

$$B \equiv A\cos\left(\frac{2\pi\theta}{T}\right),\ C \equiv A\sin\left(\frac{2\pi\theta}{T}\right) \tag{37}$$

and fit the equivalent model

$$\phi(t,T,B,C) = B\sin\left(\frac{2\pi t}{T}\right) + C\cos\left(\frac{2\pi t}{T}\right). \tag{38}$$

(If the value of T is known, the second form is linear in the unknown parameters.) We can convert estimates $\hat{T}$, $\hat{B}$, and $\hat{C}$ to estimates of amplitude and phase by

$$\hat{A} = +\sqrt{\hat{B}^2 + \hat{C}^2},\quad \hat{\theta} = \frac{\hat{T}}{2\pi}\tan^{-1}\left(\frac{\hat{C}}{\hat{B}}\right). \tag{39}$$

We can convert uncertainty estimates $\sigma(\hat{T})$, $\sigma(\hat{B})$, and $\sigma(\hat{C})$ by

$$\sigma(\hat{A}) = \frac{1}{\hat{A}}\left[\hat{B}^2\sigma^2(\hat{B}) + \hat{C}^2\sigma^2(\hat{C}) + 2\hat{B}\hat{C}\hat{V}(\hat{B},\hat{C})\right]^{1/2} \tag{40}$$

and

$$\sigma(\hat{\theta}) = \frac{\hat{T}}{2\pi\hat{A}^2}\left[\hat{B}^2\sigma^2(\hat{C}) + \hat{C}^2\sigma^2(\hat{B}) - 2\hat{B}\hat{C}\hat{V}(\hat{B},\hat{C})\right]^{1/2} \tag{41}$$

where $\hat{V}(\hat{B},\hat{C}) = \text{covariance}(\hat{B},\hat{C})$ is the appropriate off-diagonal element of

$$\hat{\mathbf{V}} \approx \frac{\text{SSR}}{m-n}\left[\mathbf{J}^T(\hat{\alpha})\mathbf{J}(\hat{\alpha})\right]^{-1}. \tag{42}$$

Table 2 gives the estimates and diagnostics for nonlinear fits of the four models

$$\phi(t,\alpha) = \alpha_1 + \alpha_2\begin{Bmatrix} t-t_0 \\ (t-t_0)^2 \\ \exp[\hat{\beta}(t-t_0)] \\ \exp[\alpha_3(t-t_0)] \end{Bmatrix} + \alpha_5\sin\left(\frac{2\pi t}{\alpha_4}\right) + \alpha_6\cos\left(\frac{2\pi t}{\alpha_4}\right), \tag{43}$$

with $\hat{T} = \hat{\alpha}_4$ and $\hat{A}$, $\hat{\theta}$ gotten from $\hat{\alpha}_4$, $\hat{\alpha}_5$, $\hat{\alpha}_6$ via Equation 39. Figure 4 shows plots of the first three fits, with the plot of the fourth again omitted to reduce clutter. It fell between the quadratic and the exponential, but closer to the former. Note the statistical significance of all the amplitude estimates, and ignore the apparent insignificance of the phase estimates because $\theta^* = 0$ is not prohibited. The last row gives the u-values for testing the null hypothesis, H_0: $\alpha_4^* = \alpha_5^* = \alpha_6^* = 0$, which is rejected in every case because $F_{0.95}(3, 141) = 2.6688$ and $F_{0.95}(3, 140) = 2.6692$.

Comparing models 3 and 4 gives $u = 14.609 > F_{0.95}(1, 140) = 3.9087$, so $\hat{\alpha}_3$ significantly reduces the SSR. This indicates that if the warming is exponential, the rate is significantly smaller than that of the fossil-fuel emissions. On the other hand, comparing models 2 and 4 gives $u = 0.2073 < F_{0.95}(1, 140)$, which implies that the additional parameter $\hat{\alpha}_3$ does not significantly reduce the SSR. This is not solid evidence against exponential warming. Remember that all these tests are based on the local quadratic approximation given by Equation 31.

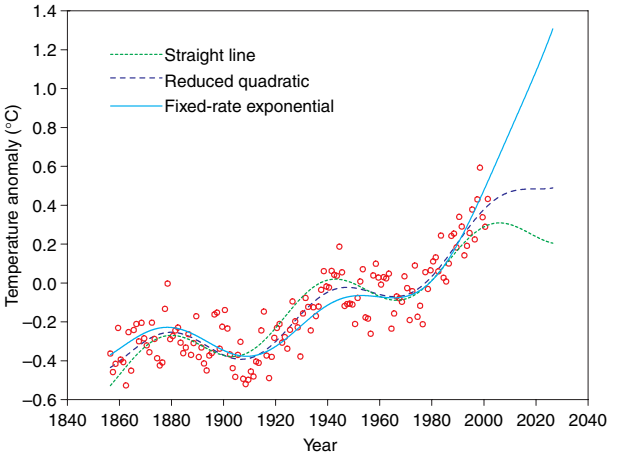

Figure 4. Five-parameter nonlinear least-squares fits to the annual global average temperature anomalies.

The previous fits do not constitute a discovery of the approximately 63-year cycle. In 1963, J.M. Mitchell Jr. found evidence for "a rhythm somewhere between 60 and 90 years in period,"[5] and in 1994, Michael Schlesinger and Navin Ramankutty reported an oscillation of 65 to 70 years.[6] The residuals for the fits also exhibit evidence for shorter period cycles that other observers have noted. We will explore those possibilities in the next installment using a simplified and improved nonlinear least-squares algorithm. CiSE

Acknowledgments

I thank Anastase Nakassis for suggesting several improvements to this manuscript.

References

1. B.W. Rust, "Fitting Nature's Basic Functions Part I: Polynomials and Linear Least Squares," *Computing in Science & Eng.*, vol. 3, no. 5, Sept./Oct. 2001, pp. 84–89.
2. B.W. Rust, "Fitting Nature's Basic Functions Part II: Estimating Uncertainties and Testing Hypotheses," *Computing in Science & Eng.*, vol. 3, no. 6, Nov./Dec. 2001, pp. 60–64.
3. G. Marland, T.A. Boden, and R.J. Andres, "Global, Regional, and National CO_2 Emissions," *Trends: A Compendium of Data on Global Change*, Carbon Dioxide Information Analysis Center, Oak Ridge Nat'l Laboratory, Oak Ridge, Tenn., 2000.
4. D.M. Bates and D.G. Watts, *Nonlinear Regression Analysis and Its Applications*, John Wiley & Sons, New York, 1988.
5. J.M. Mitchell Jr., "On the World-Wide Pattern of Secular Temperature Change," *Changes of Climate*, United Nations Educational, Scientific, and Cultural Organization, Paris, 1963, pp. 161–181.
6. M.E. Schlesinger and N. Ramankutty, "An Oscillation in the Global Climate System of Period 65–70 Years," *Nature*, vol. 367, 24 Feb. 1994, pp. 723–726.

Bert W. Rust is a research mathematician at the National Institute of Standards and Technology. His research interests include ill-posed problems, time series modeling, nonlinear regression, and observational cosmology. He received his BS in engineering physics and MS in mathematics from the University of Tennessee and his PhD in astronomy from the University of Illinois. Contact him at the Nat'l Inst. of Standards and Technology, 100 Bureau Dr., Stop 8910, Gaithersburg, MD 20899-8910; bwr@cam.nist.gov.